The Laser Tomography Adaptive Optics System of the Giant Magellan Telescope

R. Conan[1a], B. Espeland[1], K. Uhlendorf[1], M. van Dam[2], and A. Bouchez[3]

[1] Research School of Astronomy & Astrophysics, The Australian National University, Canberra, ACT, Australia
[2] Flat Wavefronts, Christchurch, New Zealand
[3] Adaptive Optics Group, Giant Magellan Telescope, Pasadena, CA, USA

Abstract. The Laser Tomography Adaptive Optics (LTAO) system of the Giant Magellan Telescope (GMT) is currently in its Preliminary Design phase. The system design goal is to deliver at K band at least 50% ensquared energy in 50 milliarcsecond squared over 80% of the sky and to achieve better than 20% Strehl ratio in J band over 60% of the sky. To reach these performance, the LTAO system will use 6 Laser guide stars (LGS) evenly located on a 35 arcsec ring centered on the science target. The measurements from the 6 Sodium LGS Shack–Hartmann wavefront sensors will drive the adaptive secondary mirror which actuator motion are derived from a minimum–mean square error tomographic reconstructor. A single infrared tip–tilt star will provide the science target tip–tilt correction. A dedicated deformable mirror in the tip–tilt path will correct the tip–tilt star wavefront aberrations. In addition to the tip–tilt sensor, a focus wavefront sensor combined with a zoom optics will keep the telescope focused on the mean altitude of the sodium layer and a high order wavefront sensor will track the so–called LGS aberrations and the system quasi static aberrations

1 Introduction

The Giant Magellan Telescope is a next generation of extremely large optical telescope. The primary mirror is made of seven large ∼ 8m diameter mirrors and the secondary mirror matched the segmented arrangement of the primary with seven Adaptive Secondary mirrors. A third retractable mirror folds the celestial beacon towards a science instrument on a Gregorian rotating platform. Three AO modes are considered for the GMT: NGSAO, GLAO and LTAO.

The Australian National University is in charge of the design of the Laser Tomography Adaptive Optics (LTAO) system. The system design goal is to deliver at K band at least 50% ensquared energy in 50 milliarcsecond squared over 80% of the sky and to achieve better than 20% Strehl ratio in J band over 60% of the sky. To reach these performance, the LTAO system will use 6 Laser guide stars (LGS) evenly located on a 35 arcsec ring centered on the science target. The measurements from the 6 Sodium LGS Shack–Hartmann wavefront sensors will drive the adaptive secondary mirror which actuator motion are derived from a minimum–mean square error tomographic reconstructor. A single infrared tip–tilt star will provide the science target tip–tilt correction. A dedicated deformable mirror in the tip–tilt path will correct the tip–tilt star wavefront aberrations. In addition to the tip–tilt sensor, a focus wavefront sensor combined with a zoom optics will keep the telescope focused on the mean altitude of the sodium layer and a high order wavefront sensor will track the so–called LGS aberrations and the system quasi static aberrations

2 LGS tomography

The performance of an LTAO system is utterly dependent upon the number of LGS and their distribution in the sky. It has been shown that LGS located on a ring around the science object gives the best wavefront reconstruction. It is then left to decide on the number of LGS and the LGS ring radius.

[a] rconan@mso.anu.edu.au

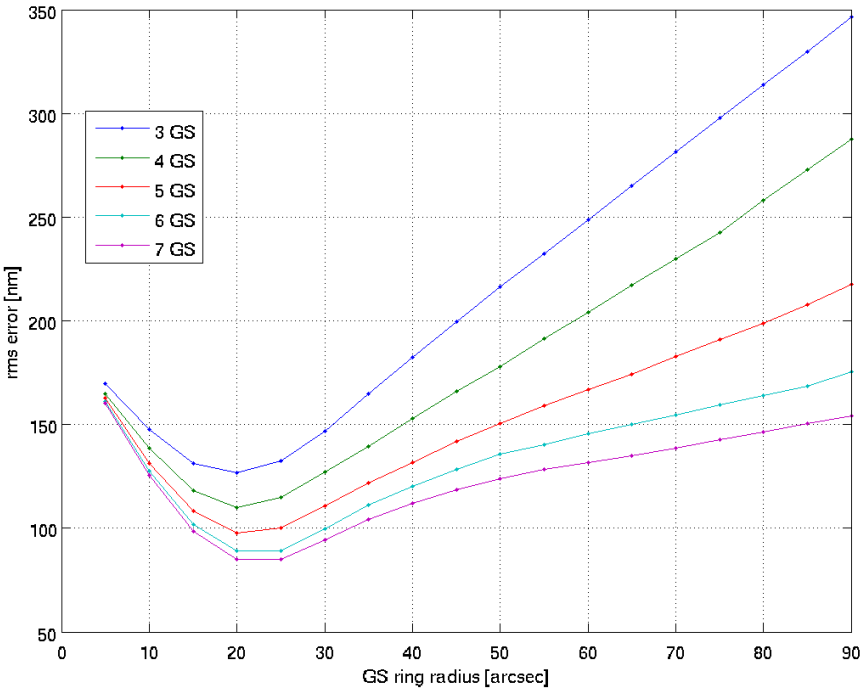

Fig. 1. Tomographic error as a function of the number of guide stars.

Fig. 1 shows the rms wavefront error as a function of LGS asterism radius for different numbers of LGSs. Increasing the number of LGSs decreases the wavefront error over the whole field of view. The radius that gives the optimal on-axis wavefront estimate ranges from 20” for 3 GSs to 25” for 7 GSs. Adding more guide stars reduces the rms error, but the gain decreases as the number of GS grows, 6 LGSs being the best trade–off between complexity and performance.

Fig. 2 plots the rms tomographic WFE as a function of the off–axis distance for 6 LGS at different asterism radii. Increasing the LGS asterism radius decreases the rms WFE off–axis at the expense of increasing the on–axis rms WFE. The off–axis error corresponds, for example, to the residual WFE experienced by the NGS TT star. The performance of the system will be also limited by the quality of the tip–tilt correction. In order to preserve a relatively good wavefront on the TT star, the LGS asterism radius as been set to 35”.

2.1 Launch telescopes location

Once the LGS constellation is decided, one must choose the location for the launch telescope(s). Three launch telescope layouts have been considered:

1. 1 launch telescope on-axis on the back of the ASM (Fig. 3 left)
2. 6 launch telescopes within the primary mirrors (Fig. 3 center)
3. 3 launch telescopes on the edge of the primary mirrors (Fig. 3 right)

Each layout will result in different patterns of elongated spots on the 6 LGS WFSs. The superimposition of the LGS spots for the 6 LGS WFSs for the 3 launch telescopes are shown in Fig. 4. This shows that the elongated spots are the same on the WFSs when the Lasers are launch from the back of the ASM whereas with the 3 launch telescopes at the edge of the telescope, the patterns of the elongated spots vary between the LGS.

Fig. 5 shows the centroiding error map per lenslet for the 3 configurations. Upper left is the noise map when launching from the back of the ASM, in the middle are the 6 WFS noise maps when

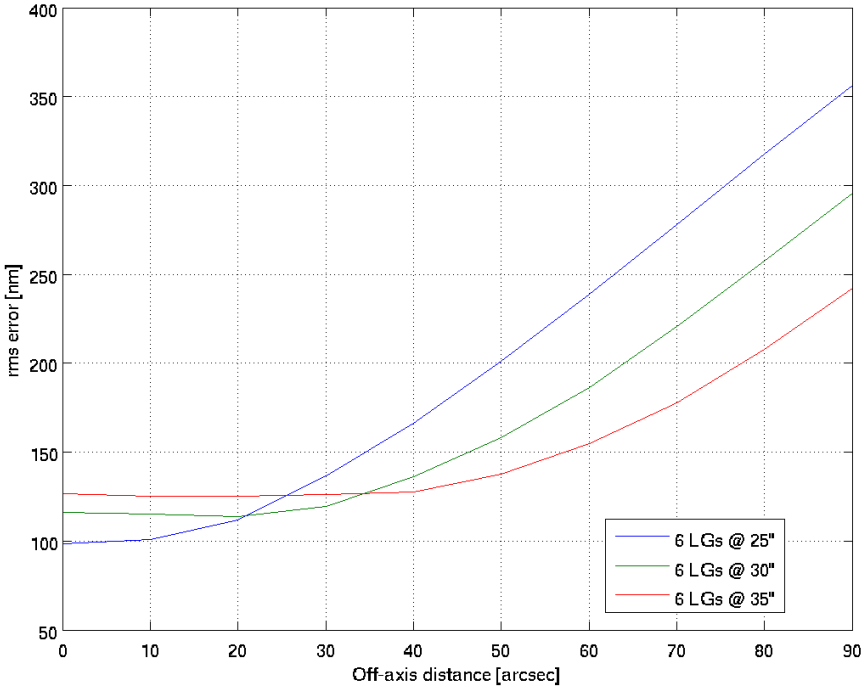

Fig. 2. Tomographic error as a function of the off-axis distance for 6 LGS at different radii.

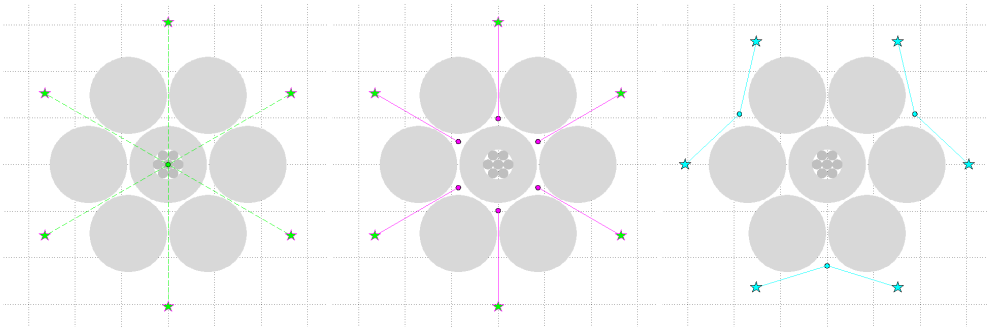

Fig. 3. 6 lasers launched from the back of the ASM, 6 launch telescopes within the primary segments and 3 launch telescopes on the primary mirror edges.

launching from within the segments and on the right are the 3 noise maps when launching from the edge. The error on the lenslets edge for the side launch Lasers is almost twice the error for the central launch Lasers. This is expected as the elongation induced by a side launch Laser is around twice the elongation induced by a central launch Laser. From Fig. 5, it may seems that the central Laser launch telescope is the most favorable layout. However, the error map should be analyzed after being processed optimally with the tomographic reconstructor.

Fig. 6 compares the tomographic measurements error for the 3 configurations. The tomographic measurement error is derived from the difference of the tomographic WFE between two LTAO systems: a noise free and infinite bandwidth one and a photon limited and finite bandwidth one. The tomographic error is estimated including the noise covariance matrix in the MMSE estimator. The noise covariance matrix model takes into account the spot elongation and the spot radial orientation with a point of origin at the launch telescope location. There is almost no difference between the measurements WFE for the 3 cases. As shown in Fig. 7, launching from the edge can even give a

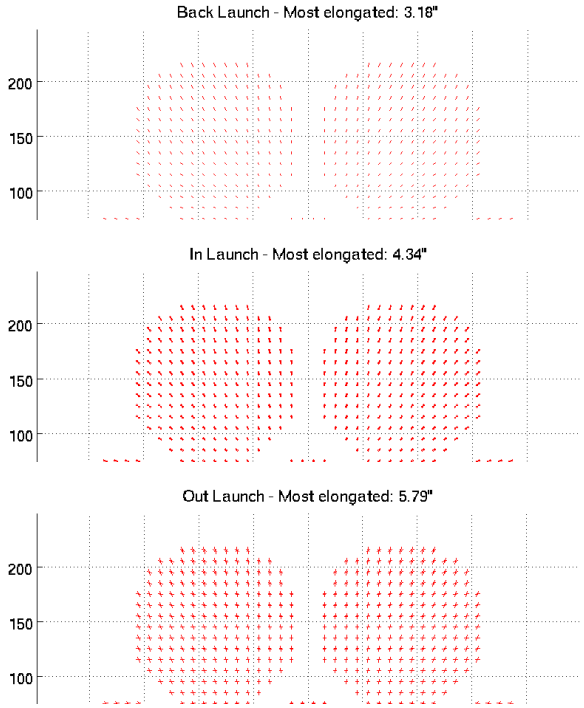

Fig. 4. LGS WFS spot elongation for one launch telescope on the back of the ASM, LGS WFS spot elongation for six launch telescopes within the segment primaries and LGS WFS spot elongation for three launch telescopes on the primary segment edges

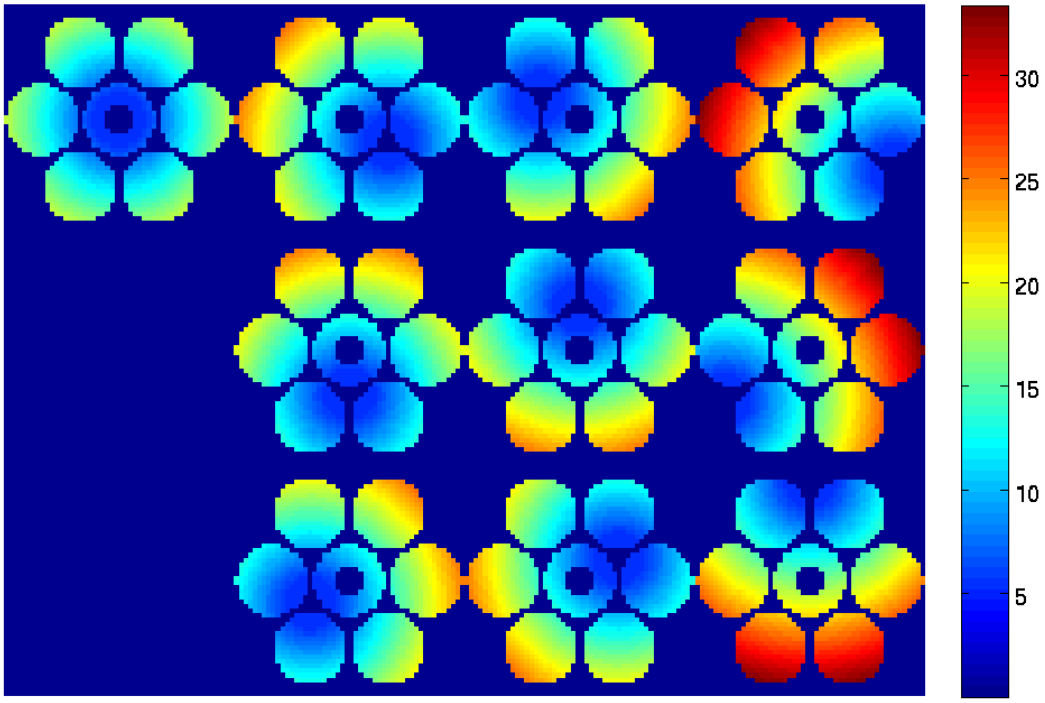

Fig. 5. LGS WFS noise maps for the 3 launch telescope configuration.

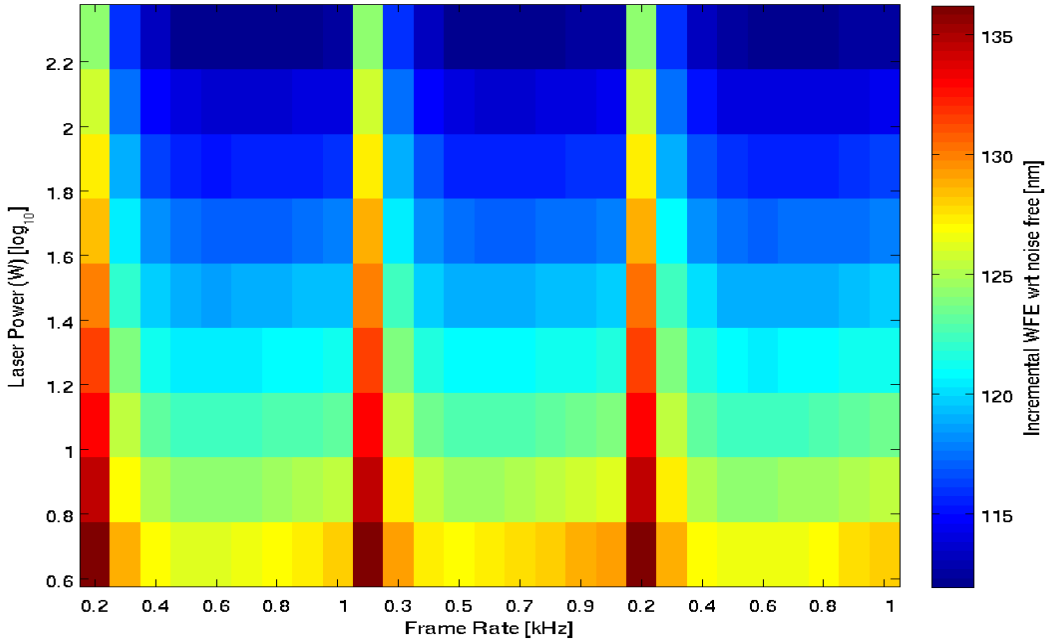

Fig. 6. LGS WFS measurement error for the 3 configurations versus the Laser power and the frame rate.

reduced WFE compared to launching from the center. This result is the consequence of i) modeling the WFS noise covariance matrix for elongated spots and ii) the elongation mitigation with different spot orientations and sizes when launching from the edge.

Hence, it has been decided to use 3 launch telescope location on the periphery of the primary. This location has also the advantage of an easier access and do not overload the ASM already complex design.

3 Tip–tilt sensing

As LGS based wavefront sensor lacks the wavefront tip–tilt component, this one needs to be retrieve from a NGS based wavefront sensor. In Fig. 8, Fig. 9, Fig. 10 and Fig. 11, isopleths of the on–axis residual jitter are compared for 4 different cases:

1. 1 R band TT star,
2. 3 R band TT star,
3. 1 K band TT str,
4. 1 AO corrected K band TT star.

For all cases, the TT sensor is a quad-cell sensor including photon–noise, read–out noise and sky background. Unsurprisingly, 3 R band seeing-limited TT stars perform better than a single seeing-limited R or K band TT star, confirming the previous results. But the best performance is obtained with 1 AO corrected K band TT star. The reason for the better performance of an AO corrected K band TT star is due to the diffraction limited spot size (19mas) compared to a seeing limited spot size (0.5”) for the other cases. The smaller the spot, the more sensitive and less noisy the centroid estimate. For this reason, we prefer to use diffraction-limited infrared stars to seeing-limited visible stars. It is found that a single AO-corrected star just meets the sky coverage requirements. Adding a second star would significantly improve performance at a cost of increased complexity. Adding a second star is relevant only if the TT jitter induced by the wind shake and instrument vibrations is controlled at better than a milli-arcsecond.

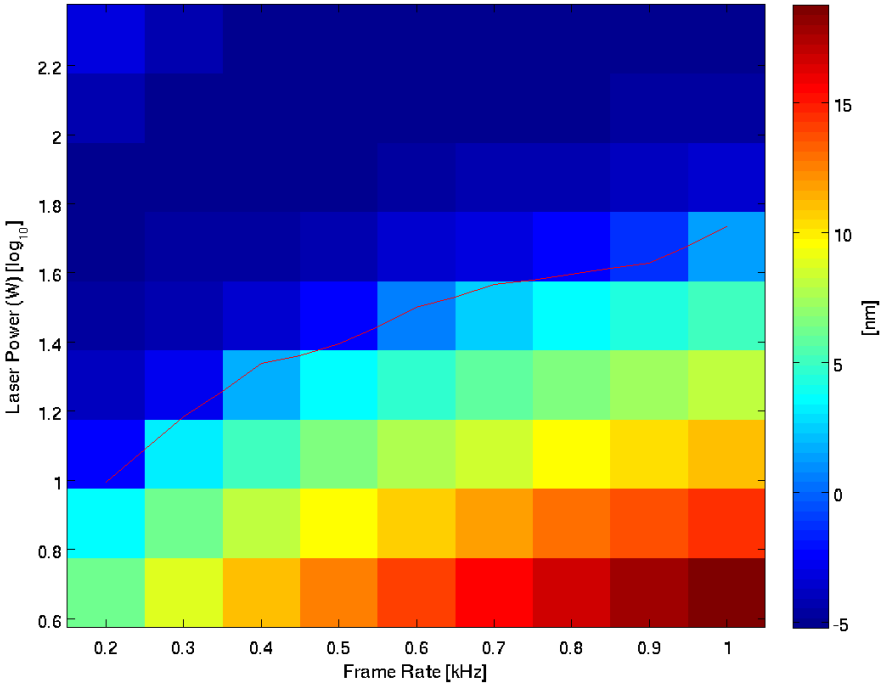

Fig. 7. Difference between the central and edge Laser launch WFS measurement error versus the Laser power and the frame rate.

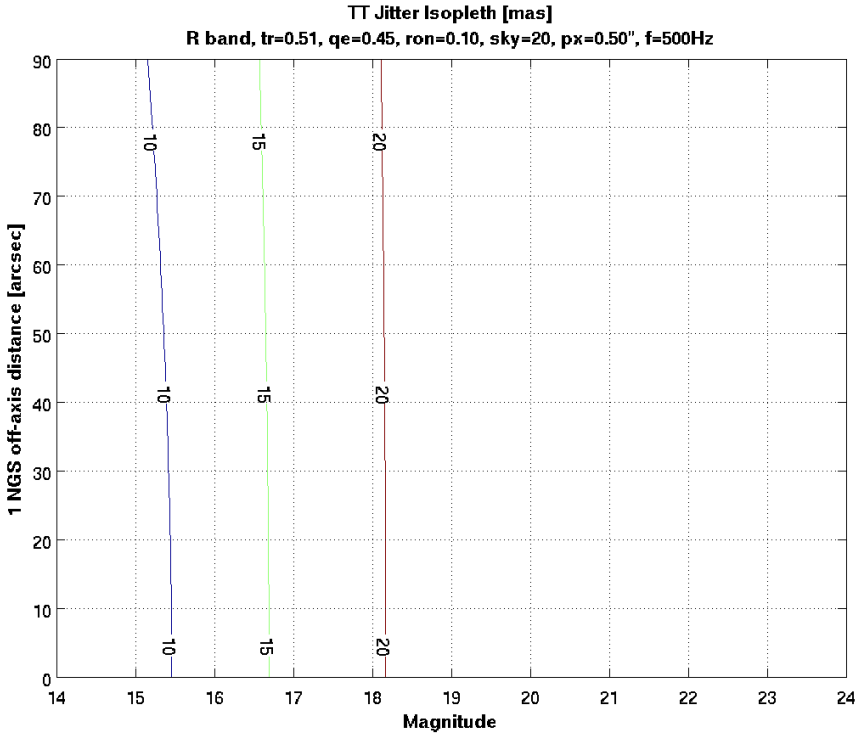

Fig. 8. Tip-Tilt Tomography with 1 R band TT star.

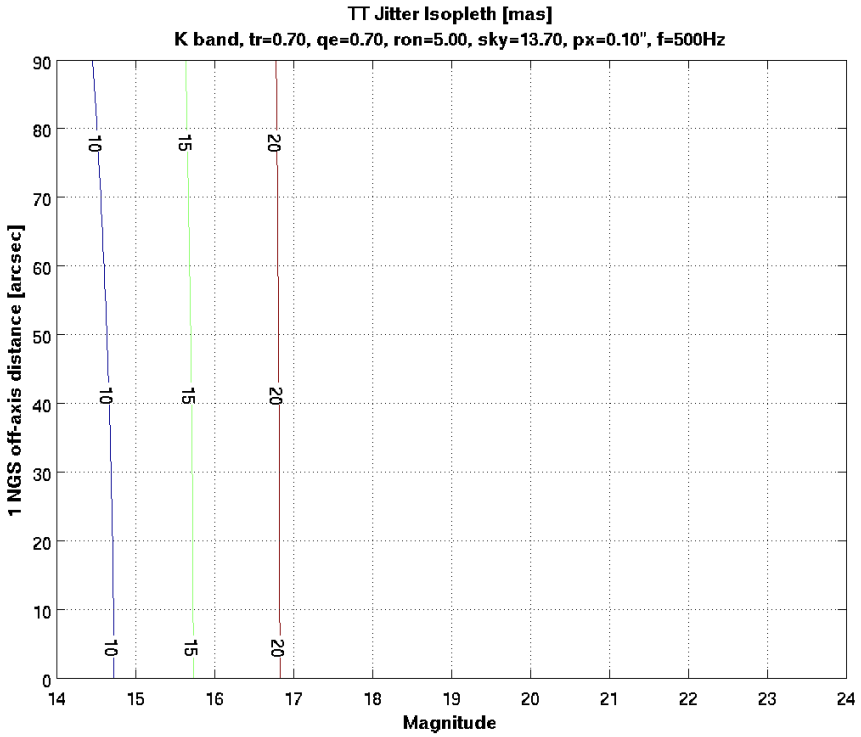

Fig. 9. Tip-Tilt Tomography with 1 K band TT star.

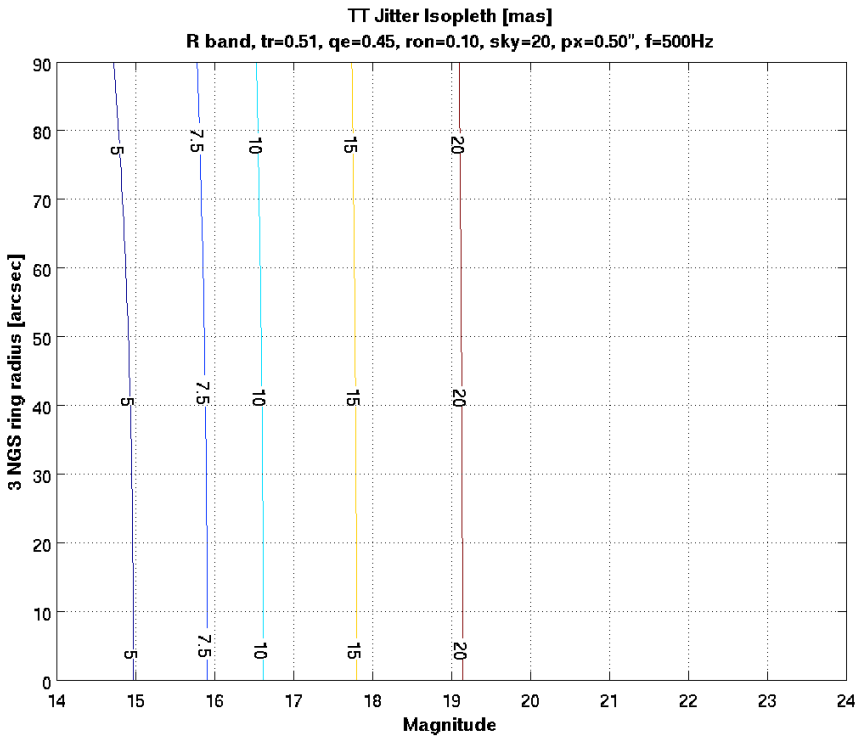

Fig. 10. Tip-Tilt Tomography with 3 R band TT stars.

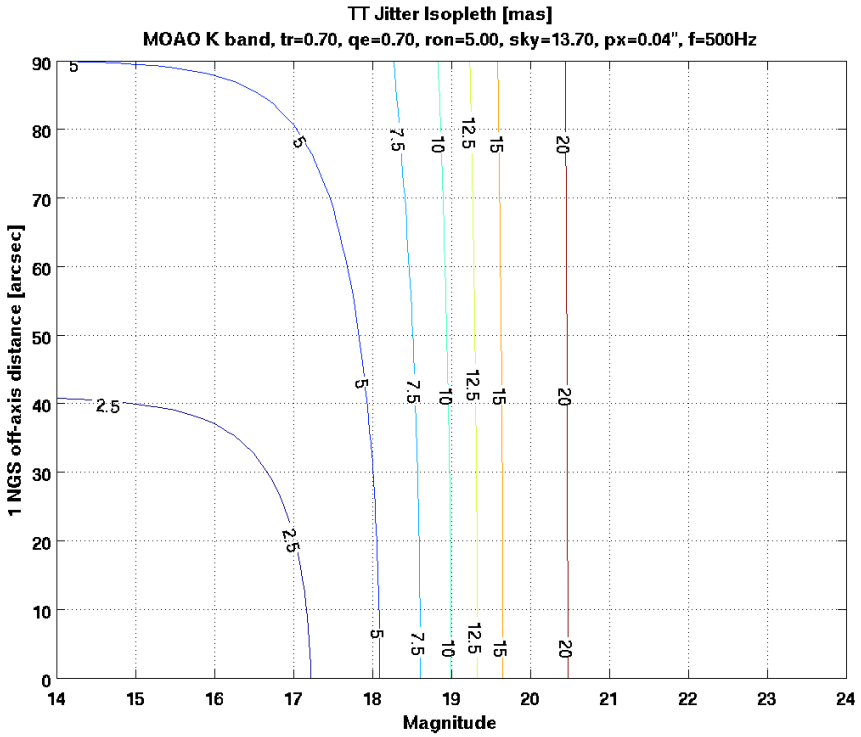

Fig. 11. Tip-Tilt Tomography with 1 AO corrected K band TT star.